First-principles investigations of electronic and magnetic properties of $SrTiO_3$ (001) surfaces with adsorbed ethanol and acetone molecules

Waheed A. Adeagbo,* Guntram Fischer, and Wolfram Hergert
Institut für Physik, Martin-Luther-Universität Halle-Wittenberg, Von-Seckendorff-Platz 1, D-06120 Halle, Germany
(Received 16 February 2011; revised manuscript received 4 April 2011; published 17 May 2011)

First-principles methods based on density functional theory are used to investigate the electronic and magnetic properties of molecular interaction of the TiO_2 terminated $SrTiO_3$ (100) surface with ethanol or acetone. Both the perfect surface and the surface with an oxygen or a titanium vacancy in the top layer are considered. Ethanol and acetone are preferentially adsorbed molecularly via their respective oxygen atom on top of the Ti atom on the perfect surface. In case of an oxygen vacancy the adsorption of ethanol or acetone occurs directly on top of the vacancy and does not significantly affect the magnetism caused by the vacancy. In the case of a titanium vacancy both adsorbates occupy positions above Ti atoms. During this adsorption process the ethanol molecule dissociates into a CH_3CO radical and three hydrogen atoms. The latter form hydroxide bonds with three of the four dangling oxygen bonds around the Ti vacancy and any magnetic moment induced by the Ti vacancy is annihilated. Thus the ethanol and acetone have a different impact on the surface magnetism of the $SrTiO_3$ (100) surface.

DOI: 10.1103/PhysRevB.83.195428 PACS number(s): 81.40.Rs, 81.65.Cf, 75.70.Rf, 73.20.At

I. INTRODUCTION

Strontium titanate $SrTiO_3$ (STO) is one of the perovskite oxides which is basically an insulator with a band gap of 3.2 eV at 25°C.[1] Its surfaces have attracted a considerable amount of attention due to their potential applications in photocatalysis, as dielectric materials in capacitors, as a high-temperature oxygen sensor, as well as substrate for high-T_c superconductors.[2–12] The understanding and improving of molecule-surface linkages of organic molecules with oxide surfaces is an important step toward the development of, for example, dye-sensitizing devices and the catalysis of diverse organic reactions.[13,14] Many theoretical and experimental studies have been carried out for $SrTiO_3$ (001) surfaces with water as an adsorbate on perfect, stepped, or reduced surfaces in order to identify the catalytic active sites on the surface.[15–18] Recently theoretical investigations have been published using other molecules such as methanol molecules (CH_3OH),[19] acetaldehyde (CH_3CHO),[20] CO,[21] NO,[22] and oxygen adatoms.[23]

Like other substrates, STO is usually ultrasonically and chemically cleaned in pure water, acetone, ethanol, or KOH solution in order to remove any trace of impurities which might contaminate the sample during the experiment. Khalid *et al.*[24] recently studied the effect of surface cleaning on the magnetic properties of MgO, $MgAl_2O_4$, $SrTiO_3$, $LaAlO_3$, and ZnO substrates. They found that the ferromagnetic-like response of the $SrTiO_3$ substrate was enhanced after ultrasonic cleaning in ethanol, while ultrasonic cleaning in acetone led to a vanishing ferromagnetic response. The repeatable "chemical" switching of the magnetization was attributed to the complex surface structure of STO. A similar observation has been reported for HNO_3 etching of Al_2O_3, reducing or removing the ferromagnetic signal from such substrates.[25,26]

Therefore, in view of the difficulty to interpret the observed changes of the magnetic state by chemical treatment we studied the interaction of two prototypic organic molecules, ethanol and acetone, with the TiO_2 terminated $SrTiO_3$ (001) surface. This was done by applying density functional theory (DFT) to investigate the electronic structure and magnetic properties that can be associated with the possibly experimentally occurring adsorption of these molecules to the TiO_2 terminated surface of STO. However, one has to keep certain limiting factors in mind. Besides neglecting the SrO termination of the STO surface, this is most notably the lack of detailed information about the experimental structure. This is why one can, in principle, not expect to find a complete and satisfactory explanation of the experimental results, but rather possible mechanisms and also processes that can possibly be excluded.

The paper is organized as follows. Section II describes the details of our DFT calculations and parameters obtained from the calculations of the bulk which were later used to describe the surface geometry and the electronic structure as well as the magnetic properties. This is followed by Sec. III, in which the results for the $SrTiO_3$ (100) surface, perfect and with defects, without adsorbates (Sec. III A), for the perfect surface with ethanol or acetone adsorption (Sec. III B), for the surface with defects under ethanol adsorption (Sec. III C), as well as for the surface with defects under acetone adsorption (Sec. III D) are discussed. The paper closes with a final discussion in Sec. IV and a summary and a conclusion in Sec. V.

II. COMPUTATIONAL DETAILS

All our calculations were performed by applying the pseudopotential method based on density functional theory (DFT) in the generalized gradient approximation[27–29] using the spin polarized mode. This was carried out with the Vienna *ab initio* simulation package[30,31] using the projector augmented-wave method.[32] Due to the well-known problems of standard DFT in describing strongly correlated systems, we used the GGA+U method for the treatment of the partly occupied 3d orbitals of Ti. In particular, we applied the on-site Coulomb correlation energy correction $U = 8.5$ eV with a J value of 1.0 eV to it. By doing so we obtained a reasonable band gap of 2.7 eV when compared to the experimental value of 3.2 eV.[1] To rule out any effects on the results that this choice

of U might induce we checked our results for a smaller U value of 5.0 eV, while keeping $J = 1.0$ eV, and also tried the case without Hubbard corrections applied at all, that is, $U = J = 0$. If not stated otherwise, however, all results and discussions presented refer to the case $U = 8.5$ eV and $J = 1.0$ eV. The expansion of the electronic wave functions into plane waves was done using a cut-off energy of 400 eV. The iterative minimization of the charge density was conducted within the framework of the residual minimization direct inversion in the iterative subspace (RMM-DIIS) method.[33] To calculate atomic relaxations we used the gradient quasi-Newton method. We assumed that the convergence was achieved when the forces acting on the atoms did not exceed 0.001 eV Å.

For the bulk calculation, the k-point sampling of a 16×16×16 mesh within the Monkhorst-Pack special k-point scheme[34] in the Brillouin zone was chosen. With these settings the STO bulk lattice constant a was calculated to be 3.98 Å. This overestimates the experimental value which is 3.91 Å[35] and as well other theoretical works,[36] the reason for that most likely being the application of the GGA+U. Using this lattice constant the STO (001) surfaces with TiO_2 termination on both sides were modeled by a periodic slab shown in Fig. 1.

It is made up of a 2×2 surface unit cell which is periodic along x and y directions. For convergence testing this was as well increased to 3×3 in order to reduce the monolayer coverage of the adsorbed molecule. One slab contains altogether nine atomic planes consisting of five TiO_2 and four SrO layers alternately stacked along the z axis normal to the surface. We did not notice any significant change in our results for the adsorbate-free surface by increasing the atomic planes to 18. The vacuum region is about 24.8 Å thick (without ethanol or acetone), corresponding to about 6.4 lattice constants. This is large enough to accommodate the ethanol or acetone adsorbate and to ensure convergence of the results. The three central layers were settled in a fixed position, and the other three layers on the two sides of the vacuum were allowed to relax symmetrically along the z axis (see Fig. 1). The initial positions of the adsorbate molecules for relaxation were kept at positions A, B, and X, that is, on top of oxygen (O), titanium (Ti), and the hollow site above the Sr atom in the second plane, respectively. The vacancy defects were later created at O and Ti sites, V_O and V_{Ti}, respectively, and then relaxations of the adsorbates on these defected sites in addition to A, B, and X were performed. The ground-state calculations for the 2×2 (3×3) surface unit cell were done using a 6×6×1 (4×4×1) k mesh within the Monkhorst-Pack special k-point scheme.[34]

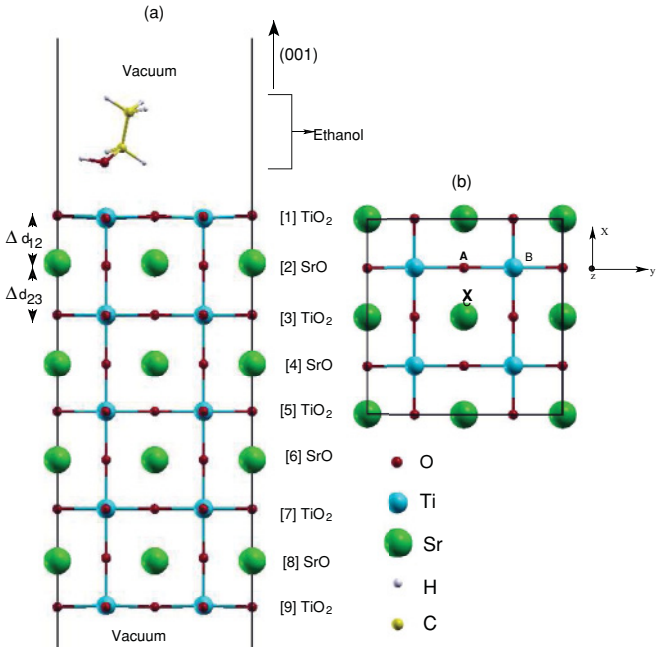

FIG. 1. (Color online) (a) The supercell geometry of the STO slab along the (100) plane showing the alternating layers of TiO_2 and SrO with TiO_2 terminations and an adsorbate molecule on top. (b) The marked points A, B, and X are the initial positions on which the adsorbate molecules are placed for relaxation. Later the defect vacancies are created at A and B, then referred to as A′ and B′, respectively.

In order to characterize the stability of an adsorbate in a region on the surface, we calculated the adsorption energy E_{ads} via

$$E_{ads} = E_{slab+adsorbate} - E_{slab} - E_{adsorbate}, \quad (1)$$

where $E_{slab+adsorbate}$ and $E_{adsorbate}$ are the calculated total energies of the slab with ethanol (acetone) on it and of isolated ethanol (acetone) adsorbate in the gas phase, respectively. Thus a negative value of E_{ads} corresponds to a preference for ethanol (acetone) adsorption on the surface.

III. RESULTS AND DISCUSSION

As mentioned earlier, the relaxation of the bulk STO yields a lattice constant of $a = 3.98$ Å, and the energy band gap is 2.7 eV. The latter can be seen in the density of states (DOS) of bulk STO in Fig. 2. As found in other previous *ab initio* calculations[37] the Ti $3d$ orbitals hybridize with the O $2p$ ones. This holds for the occupied as well as for the unoccupied states.

Both the ethanol and acetone molecules used in our calculations were relaxed in a big cell. The resulting geometrical parameters from the relaxation are consistent with those obtained from Gaussian-type orbitals density functional theory calculations[38] and experimental values.[14] Generally the error between the calculated and experimental values for the distances and angles between two atoms forming a bond was less than 1%.

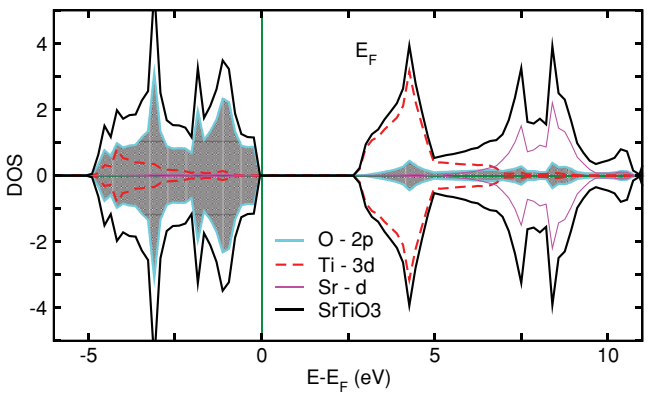

FIG. 2. (Color online) Total and site projected electronic density of states of bulk $SrTiO_3$.

TABLE I. Summary of the changes in the interlayer spacings Δd_{ij} and of the surface rumplings s of the O atoms of the three investigated clean surfaces. The rumpling measures the outward displacement of the surface O atoms relative to the first layer metal atoms. NN refers to nearest neighbor atoms of defects, NNN to second nearest neighbors. For each case the largest absolute values are given.

Surface		Δd_{12} (Å)	Δd_{23} (Å)	s (Å)
Perfect		−0.05	0.05	0.06
V_O	NNN	−0.04	0.06	0.06
V_{Ti}	NNN	−0.05	0.03	0.06
V_O	NN	0.11	0.01	−0.22
V_{Ti}	NN	0.08	−0.10	0.04

A. No adsorbates at the perfect surface or at the surface containing defects

In order to describe the results from the surface relaxation we define Δd_{ij} as the change in the interlayer spacing between layers i and j with respect to the bulk value $d_0 = 1.99$ Å. Thus, Δd_{12} is the change between the terminating TiO_2 layer and the second layer which is SrO, and Δd_{23} is the change in spacing between the second (SrO) and the third layer (TiO_2) (see also Fig. 1 for illustration). Note that Δd_{ij} is based on the positions of the relaxed metal ions. A summary of the Δd_{ij} for all three investigated clean surfaces, that is, surfaces without adsorbates, is given in Table I.

For the bare surface with no defects and no adsorbate molecules, we obtained Δd_{12} close to −0.05 Å and Δd_{23} close to 0.05 Å, respectively. This means, in agreement with other *ab initio* calculations,[39,40] that the distance between the surface TiO_2 layer and the underlying SrO layer becomes smaller while the distance between the second and third layer increases. For the surface rumpling s, which is the upward buckling of the O atoms in the top layer with respect to the Ti atoms, we obtained the value of 0.06 Å, with the oxygen atoms relaxing towards the vacuum region. There is no induced magnetic moment (MM) on the surface after relaxation.

When the oxygen vacancy V_O or the Ti vacancy V_{Ti} are introduced to the top layer, the surface morphology is changed from that of the bare clean surface. A slight gradient in the surface plane is observed as Δd_{ij} and s of nearest neighbors (NN) of the defect site and of regions further away from it differ from each other. In particular, the amplitudes of the surface rumplings are bigger near the defect site, which can be seen in Table I as well. For NN of V_O or V_{Ti}, we get $\Delta d_{12} \simeq 0.1$ Å (see Table I), while the obtained values for regions further away from the defect site are close to that of the perfect surface. This can be explained by the ionic character of the STO. The V_O (V_{Ti}) induces electrons (holes) on its Ti (O) neighbors in that layer, which therefore gain a relative negative (positive) charge. These are therefore repelled from the ions underneath in the SrO layer, which are the negatively (positively) charged O (Sr) ions. For the change in the next interlayer spacing Δd_{23} one can see as well from Table I that its values for non-NN of the defect are close to that of the perfect surface, whereas the d_{23} increase becomes smaller for NN of the defects.

The rumpling s is relatively constant except for the NN case around the oxygen vacancy V_O, where it is strongly increased.

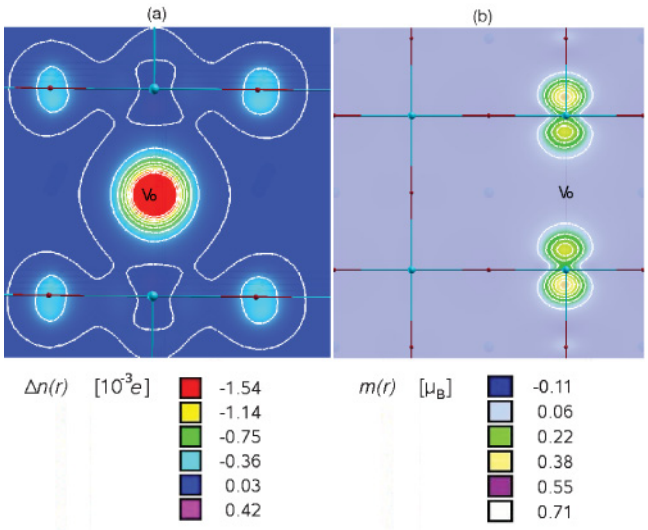

FIG. 3. (Color online) (a) Charge density difference between the perfect and oxygen vacancy defective STO slab, $\Delta n(\vec{r}) = n(\vec{r})_{V_O} - n(\vec{r})_{\text{Perf}}$. V_O is in the center. (b) Spin density distributions around V_O on the STO surface with TiO_2 termination.

However, care must be taken for this value as, due to the limited size of the unit cell, the corresponding atom is in between the two Ti atoms which are direct neighbors of the vacancy. This can be seen in Fig. 3(b). Nevertheless, the reason for the large s is once more the ionic character of the STO. The two Ti atoms nearest to V_O carry the dangling electrons that formerly occupied the O $2p$ orbitals and therefore carry a relative negative charge. This charge transfer is depicted in Fig. 3(a). Thus the anionic O atom surrounding them is repelled from them. The DOS of each of these relaxed geometrical surfaces are shown in Fig. 4. The band gap of the defect free surface is about 1.6 eV which is smaller than the bulk value in Fig. 2 due to the well-known surface band gap reduction. The overall TiO_2 surface layer is insulating and there is no induced magnetic moment for the defect-free TiO_2 surface termination.

In the case of the oxygen vacancy at the surface one sees in Fig. 4 that states appear in the gap, which is therefore reduced to approximately 0.7 eV. This is mainly caused by the appearance of Ti-3d states at the bottom of the conduction band. These are created by the dangling Ti electrons formerly occupying the $2p$ states of the now missing oxygen. The O vacancy thus causes a charge transfer from the site of the vacancy to the NN Ti atoms[41] which is illustrated in Fig. 3.

The two dangling electrons of the these two neighboring Ti atoms are spin polarized as can be seen in the charge difference and the real spin density distribution in the supercell containing the oxygen vacancy in Fig. 3(b). The resulting magnetic moment in the system is MM $= 2.0\,\mu_B$, as given in Table II.

The DOS plots in Fig. 4 also reveal the asymmetry between the spin↑ and spin↓ states. It should be noted that applying $U \leqslant 5$ eV (not shown) reduces the exchange splitting and thus creates half-metallic behavior. This is in agreement with previous calculations, where such behavior was found for oxygen vacancies in bulk STO.[36]

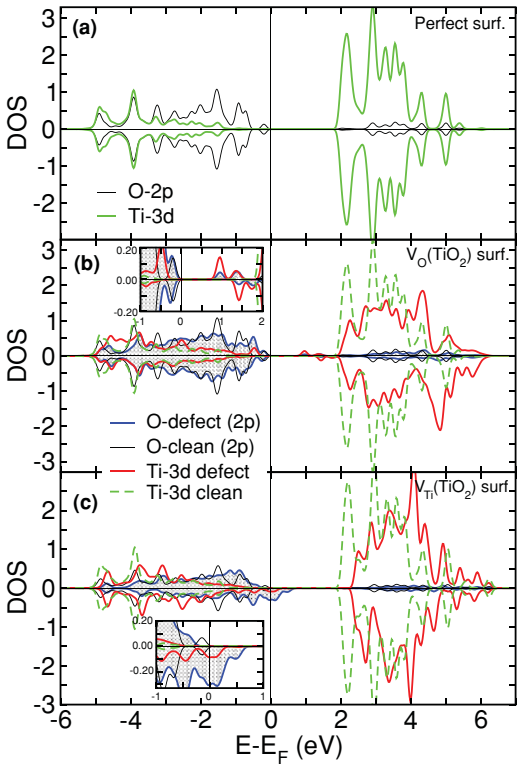

FIG. 4. (Color online) Density of states of TiO_2 surface in STO (001). Given are the DOS for the relaxed clean surface (a), for the oxygen vacancy V_O (b), and for the Ti vacancy V_{Ti} (c).

In case of the surface Ti vacancy the system becomes magnetic as well and additionally half metallic, which can be seen in the DOS in Fig. 4(c). This result agrees with predictions about Ti vacancies in bulk STO.[36] It is as well consistent with theoretical studies about cation vacancies in other formally nonmagnetic oxides, for example, ZnO,[42,43] CaO,[44] and MgO.[45,46] The induced MM is 3.77 μ_B. This value of approximately 4 μ_B corresponds to the four holes induced by V_{Ti}. The fact that it is not integer is due to the relaxation around the defect and the resulting broadening of the defect states at the Fermi level.[47] The MM is distributed over the four surrounding nearest neighbor (NN) oxygen atoms in the top layer with 0.58 μ_B per O atom. The NN O in the SrO plane carries MM = 0.27 μ_B. The magnetization of the next nearest neighboring (NNN) O atoms in the top layer is already small, MM = 0.27 μ_B per O, but this value should be taken with care due to the limited size of the surface supercell in the x and y direction. The magnetic moment on the Ti atoms nearest to the vacancy is MM = 0.01 μ_B and that on the Sr atom in the SrO plane close to the defect is even smaller.

TABLE II. Total magnetic moments (MM) induced in the surface for the three investigated systems without adsorbates.

	No Defect	V_O	V_{Ti}
MM (μ_B)	0.00	2.00	3.77

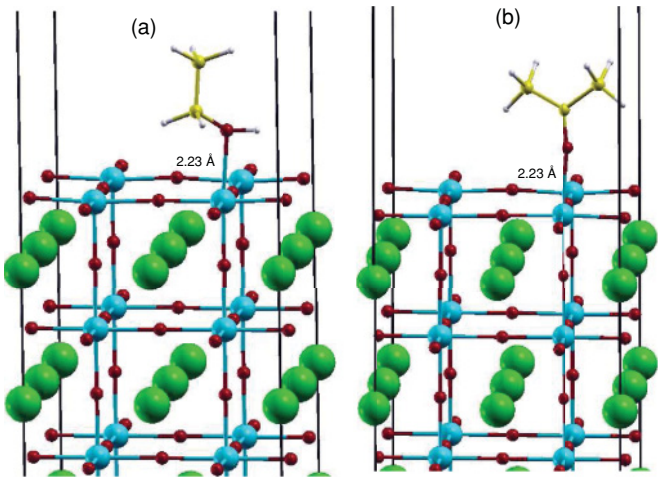

FIG. 5. (Color online) Relaxed ground-state geometry of $SrTiO_3$ (001) slab with (a) ethanol and (b) acetone molecules preferentially adsorbed at the Ti site of TiO_2 termination.

B. Adsorption at the perfect surface

For the adsorption of ethanol and acetone on the perfect surface we considered three possible starting regions for the adsorbates as indicated in Fig. 1. These are either directly on O (A), on Ti (B), or in the hollow region X above the Sr atom in the layer underneath. We found that the lowest energy is obtained when ethanol or acetone are located on top of Ti of the TiO_2 surface. This result is in fact obtained by relaxing any of the three initial configurations. The corresponding ground state structures are shown in Fig. 5. There one sees as well that the molecular bonding occurs via an O atom of the adsorbate with a bond length of 2.23 Å in both cases. The estimated adsorption energies of ethanol were found to be −0.75 eV for ethanol and −0.70 eV for acetone. The effect of the adsorbates on the DOS of the perfect surface is shown in Fig. 6.

There one sees that neither of them induces any magnetic moment on the surface or is magnetic itself. The adsorbates have only a small effect on the Ti atom which they are closest to, and no strong hybridization between the latter and the O of the adsorbate is found, thus suggesting only a weak coupling. Furthermore, the effect on the O p electrons is more or less negligible. Interesting to note is the fact that acetone induces a gap state. Such dissociation and resulting emergence of gap states has been observed for other systems before.[48] Besides its impact on the material properties and possible applications, this provides a way to gain insight into the chemical composition of the adsorbate on the surface experimentally, for example, by using spectroscopy.

C. Ethanol adsorption at the surface containing defects

Like in the previous section we considered the starting regions for the adsorption process as indicated in Fig. 1, that is, directly on O (A), on Ti (B), and in the hollow region X above the Sr atom in the next layer. In addition, starting sites A′ on top of V_O and B′ on top of V_{Ti} were examined. Again we allowed the relaxation of the entire slab surface-adsorbate system. For the oxygen vacancy the energetically most favorable position of the ethanol molecule to be is shown in Fig. 7. There one

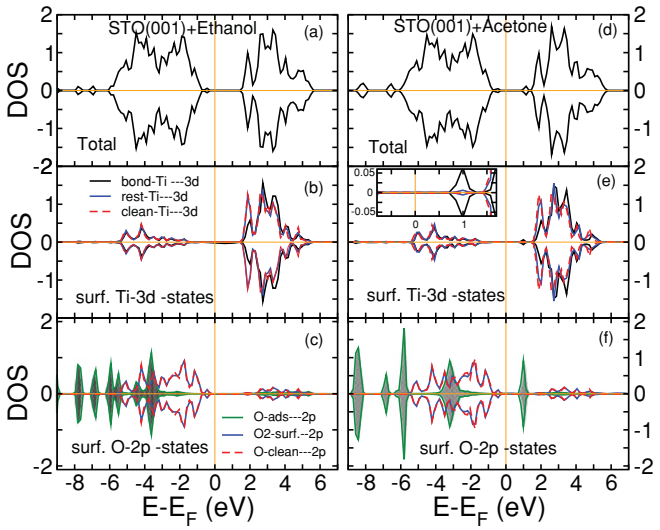

FIG. 6. (Color online) Total and partial DOS of the ground-state structures shown in Fig. 5. Top row: Respective total DOS with ethanol (a) and acetone (d) as adsorbate. Middle row: Ti 3*d* states [(b) ethanol, (e) acetone] where bond-Ti refers to the Ti that forms the "bond" between the surface and the adsorbate, rest-Ti means the remaining Ti atoms. For comparison the partial DOS of the Ti atoms in the clean surface is shown as well. Bottom row: Oxygen 2*p* states [(c) ethanol, (f) acetone] of the O of the adsorbate (O-ads), of the O atoms of the defective surface (O2-surf), and for comparison of the O atoms of the clean surface.

sees that the OH functional group is located above the site of the removed oxygen atom (A′). The reason why it is not located directly in the surface are the positively charged H atoms being repelled from the likewise positively charged Ti atoms. The respective adsorption energy is −1.20 eV, as given in Table III. Thus, from an energetical point of view, one can say that an oxygen vacancy slightly enhances the adsorption of ethanol.

The DOS of the surface with the oxygen vacancy and the ethanol adsorbate is given as well in Fig. 7. It shows that the effect of the defect is localized around its nearest Ti and O atoms, as the partial DOS of these atoms that are further away are almost identical to those of the perfect and clean surface.

TABLE III. Adsorption energies at various positions of adsorbate molecules on the TiO_2 surface of $SrTiO_3$ (001). V_O and V_{Ti}, respectively, denote the oxygen and titanium vacancy on the surface.

		E_{ads} (eV)	
Surface	Adsorbate	Above Ti	Above Defect
Perfect	Ethanol	−0.75	–
V_O	Ethanol	−0.78	−1.20
V_{Ti}	Ethanol	−0.91[1] / −9.36[2]	−7.00
Perfect	Acetone	−0.70	–
V_O	Acetone	−0.68	−0.96
V_{Ti}	Acetone	−0.69	−0.30

[1]Value obtained if relaxation is started with ethanol on top of Ti atom, no dissociation occurs.

[2]Value obtained after structural relaxation in two steps and dissociation of the H atoms as described in the text.

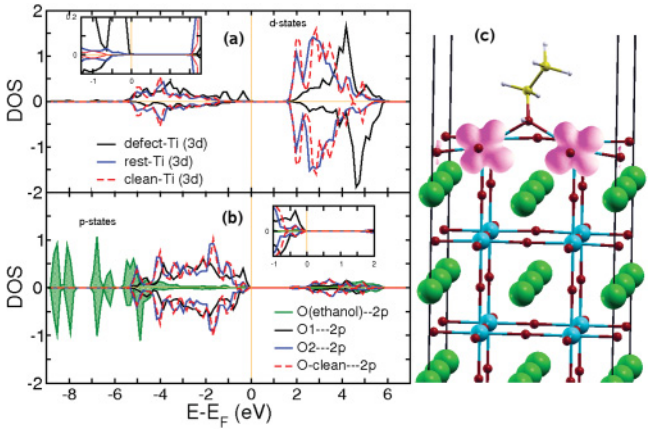

FIG. 7. (Color online) (a) Partial DOS showing the *d* states of the surface with V_O and ethanol, subdivided into those from the NN of V_O (defect-Ti), all other Ti atoms (rest-Ti), and for comparison the Ti from the perfect and clean surface (clean-Ti). (b) DOS showing the O *p* states of the ethanol molecule [O(ethanol)], of the O atoms nearest to V_O (O1), of the remaining O atoms (O2), and for comparison of the perfect and clean surface (O-clean). (c) Relaxed ground-state geometry of the TiO_2 terminated STO surface containing an oxygen vacancy with ethanol above the vacant site in between the two neighboring Ti atoms. The purple isospheres represent the magnetization density.

It shows as well that, as in the case of the perfect surface, the adsorbate does not significantly interact with the surface. This can be seen from the comparison of the clean surface with V_O [Fig. 4(b)] and the respective states of the atoms nearest to the vacancy and the ethanol: no significant changes are visible. In particular, the magnetic moment is unaffected.

For the surface containing a Ti vacancy the most favorable location of the ethanol molecule is above the Ti atom. The corresponding adsorption energy is −9.36 eV. This very large value can be explained by looking at the relaxed structure shown in Fig. 8. There one sees that the molecule has lost

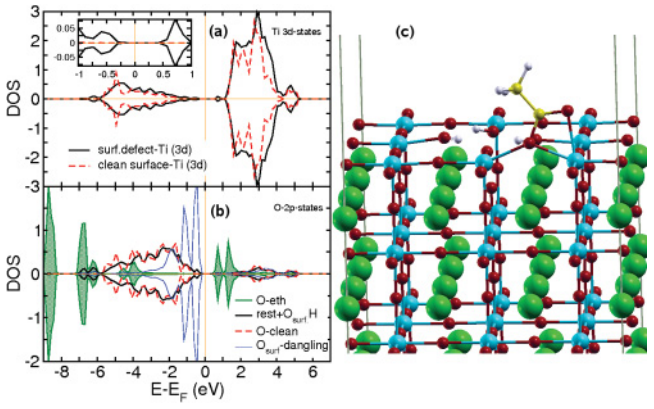

FIG. 8. (Color online) Partial density of 3*d* (a) and 2*p* (b) states of the surface containing a Ti vacancy. The holes in the O *p* orbitals are completely filled by the electrons coming from the H and from a charge transfer from the ethanol O to the O near V_{Ti}. (c) The relaxed structure of the surface. Clearly visible are the dissociated H atoms now forming, together with the C close to the surface, bonds with three of the four surface oxygens and thereby filling up *p* holes.

three H atoms which now form OH groups with the surface O atoms around V_{Ti}, which is due to the reactive nature of the dangling oxygen bonds. Their saturation results in the large energy gain. As this process fills up the p holes visible in the bottom row of Fig. 4 the magnetic moment collapses completely, the net MM in the surface cell is 0.0. This can be seen in the DOS in Fig. 8. There it is also shown that the fourth electron necessary to saturate all holes comes from the oxygen of the adsorbate. The latter shows a behavior similar to that in the case of acetone, that is, it forms gap states (see Fig. 6) after losing the three hydrogen atoms. As mentioned before, this could provide a method to experimentally verify that the calculated structure is present at the surface and responsible for the observed magnetic behavior of the sample. Finally, it is noticed that the surface becomes insulating again after the adsorption.

We mention that the structure shown in Fig. 8 is the result of starting the relaxation from position B′ above the Ti vacancy (see Fig. 1). As listed in Table III, this results in an adsorption energy of −7.00 eV, mainly caused by the dissociation described above. The energy is then further reduced by moving the remaining CH_3CO radical to position B, that is, to a place above a Ti atom and letting the system relax into equilibrium a second time. Starting the relaxation of the ethanol molecule directly on top of a Ti atom and not above the vacancy does not result in the dissociation of the H atoms. In this case the complete ethanol molecule adsorbs at the Ti atom, the resulting adsorption energy is −0.91 eV, and the magnetic moment is in principle unaffected by the adsorption.

D. Acetone adsorption at the surface containing defects

For the oxygen (titanium) deficient surface with acetone on it we again investigated the adsorption at the sites A, B, and X as well as at the O (Ti) vacant site A′ (B′), as indicated in Fig. 1. When considering V_O we found, like in the case of ethanol, the adsorption of the carbonyl group of acetone at A′, that is, right above V_O, to be the most favorable with an adsorption energy of −0.96 eV (see Table III). The distances between the O atom of the adsorbate and the two Ti atoms, 2.20 and 2.14 Å, respectively, are smaller than in the case of ethanol. This can be explained by the absence of an H atom at the bonding O atom, contrary to the OH group in the case of ethanol, where the cationic H is repelled from the equally cationic Ti atoms.

As can be seen in the DOS and in the distribution of the magnetization in Fig. 9, the magnetic moment is still mainly located on the Ti atoms nearest to V_O. However, contrary to the case of ethanol, it is also partially spread over the O atom of the acetone and its nearest carbon atom. The reason for this is again the absence of H at the bonding oxygen atom and the resulting close distance to the Ti atoms. As can be seen in the DOS in Fig. 9 this results in a strong hybridization between the p states of the O of acetone and the d electrons of the Ti atoms nearest to V_O, the consequence of which is a spin splitting of the former. The total MM in the surface cell, however, remains constant at 2.00 μ_B, and besides its spread over the adsorbate it remains localized in the close vicinity of the vacancy.

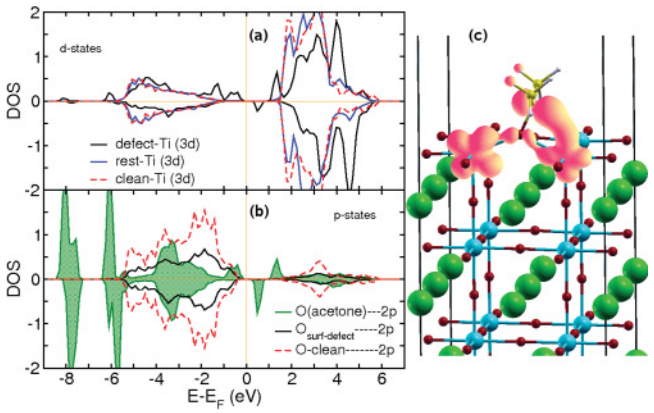

FIG. 9. (Color online) Partial DOS of the surface containing V_O for Ti (a) and O (b) electrons after acetone adsorption. Symbols and abbreviations are defined as in Fig. 7, $O_{surf-defect}$ stands for O atoms of the surface. (c) Relaxed structure of the surface. Notice the appearance of nondegenerate peaks in the gap resulting from the effect of the oxygen vacancy on the interaction between the adjacent Ti atoms and the carbonyl group. In the absence of the defect the peaks are degenerate as can be seen in Fig. 6.

The above described structural and magnetic configuration is only ≃0.1 eV lower in energy than a configuration in which the O of the acetone is located slightly closer to the surface, that is, to the site of V_O. In this case any induced magnetic moment vanishes.

When acetone is adsorbed on the surface with the Ti vacancy, the most preferable configuration is when the acetone is located on top of a Ti atom, as shown in Fig. 10. This is due to the repulsion between the O atom of the acetone and the O atoms around the vacancy. The corresponding adsorption energy is −0.69 eV. As in the case of ethanol at the Ti vacancy, the adsorbate is not as close to the surface as its O atom is slightly repelled from the surface O atoms.

The electronic structure in Fig. 10 shows that the magnetization remains strongly localized at the O atoms surrounding the Ti vacancy and is therefore nearly unaffected from the adsorption process. The total induced MM equals 3.89 μ_B which means that it is slightly, but not significantly, increased.

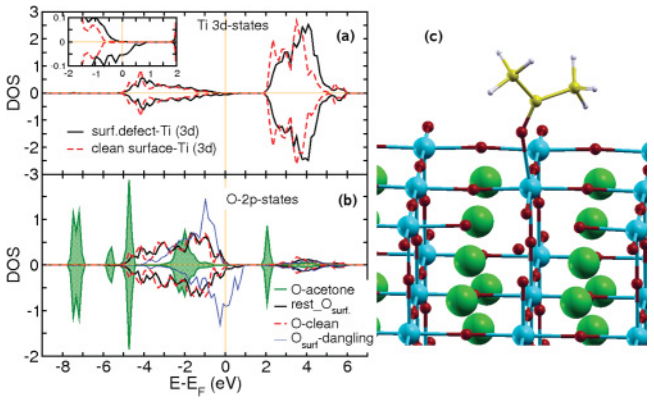

FIG. 10. (Color online) Partial DOS of the surface with V_{Ti} and an adsorbed acetone molecule located on top of Ti [as before divided into Ti 3d (a) and O 2p (b) states]. Abbreviations are equivalent to those in Fig. 8. (c) Relaxed structure of the surface.

TABLE IV. Summary of the total MM in μ_B in the surface, depending on the respective defect and adsorbate. The obtained values for a smaller Hubbard-U and for no Hubbard corrections are given as well. The first three rows with $U = 8.5$ eV summarize the results presented above. Notice the effect of ethanol on the MM of the Ti vacancy.

U (J) (eV)	Adsorbate	No Defect	V_O	V_{Ti}
8.5 (1.0)	Clean	0.00	2.00	3.77
	Ethanol	0.00	2.00	0.00
	Acetone	0.00	2.00	3.89
5.0 (1.0)	Clean	0.00	1.59	3.78
	Ethanol	0.00	2.00	0.00
	Acetone	0.00	2.00	3.11
0.0 (0.0)	Clean	0.00	1.27	3.75
	Ethanol	0.00	1.83	0.00
	Acetone	0.00	1.01	2.90

IV. DISCUSSION

The results regarding the magnetization in the surfaces are summarized in the first three rows of Table IV.

They show that the magnetic moment in the surface may depend on the adsorbate. In particular, the MM of a little less than 4 μ_B around the Ti vacancy is relatively stable under the influence of acetone, whereas it is completely annihilated by ethanol. As discussed, the latter is caused by the dissociation of the H atoms from the molecule. This suggests that the strength of the surface magnetism caused by Ti vacancies should not be significantly affected by treatment with acetone, but should reduce after treatment with ethanol. However, the opposite has been observed in experiment.[24] Therefore it could be possible that the dissociation of ethanol prevents the annihilation of donatorlike and acceptorlike defects, which has been shown to weaken defect-induced magnetism in bulk materials.[43] However, in order to be able to find accurate explanations for experimental observations it is necessary to know more about the nature of the defects present during experiments at the STO surface. Furthermore, another possible reason for surface magnetism or, in particular, an adsorbate dependent change of the surface magnetism may be stepped surfaces.

Assuming the ground state of the V_O surface to be magnetic (see remark in Sec. III D) Table IV indicates that the MM induced by an oxygen vacancy is not qualitatively and strongly affected by the kind of adsorbate and by adsorption in general. But as mentioned in that previous part the magnetic and nonmagnetic configuration for $U = 8.5$ eV have an almost identical structure and are energetically almost degenerate. The MM might therefore be rather unstable. This assumption is strengthened by the case $U = J = 0$ where structural convergence of the calculation is extremely slow and, furthermore, the result seems to be extremely sensitive to the initial configuration.

In any case, Table IV shows that the above arguments are not affected qualitatively by changing the Hubbard-U. As can be seen, the trend remain the same for a smaller value of U and as well for standard DFT, that is, applying no correlation corrections.

V. SUMMARY AND CONCLUSION

We have studied the magnetic properties of the TiO_2 terminated STO surface. We found that Ti as well as O vacancies induce magnetic moments at the surface which is nonmagnetic without defects. The magnetic moments and also the surface roughening due to the vacancies are of local character. Furthermore, we have investigated the effect of ethanol and acetone adsorbtion at the perfect and defective surfaces on the magnetic properties. We have found that neither of them induces magnetism in the perfect surface. In the case of an oxygen vacancy at the surface we have shown that both adsorbates do not affect the MM around the vacancy significantly. In the case of a Ti vacancy, however, we found adsorbate dependent behavior, as acetone adsorption does not affect the MM around the defect significantly, whereas an ethanol molecule annihilates the magnetization completely. This is due to the dissociation of the H atoms of the molecule which act as donors on the dangling oxygen electrons and thus fill up the holes responsible for the MM formation.

Thus we have shown from a theoretical point of view that the liquid used for cleaning may affect the surface magnetism of a sample. However, in order to explain particular results from experiment showing changes of the magnetism depending on the material used for the surface cleaning, more knowledge about the experimental structure of the surface is necessary.

ACKNOWLEDGMENTS

This work was financially supported by the German Research Foundation (DFG) within the SFB 762 "Functionality of Oxidic Interfaces."

*waheed.adeagbo@physik.uni-halle.de

[1] M. Cardona, Phys. Rev. **140**, A651 (1965).
[2] T. Tsumurai, K. Sogabe, and M. Toyoda, Mater. Sci. Eng. B **157**, 113 (2009).
[3] W. Menesklou, H.-J. Schreiner, K. H. Härdtl, and E. Ivers-Tiffée, Sensors Actuators B: Chem. **59**, 184 (1999).
[4] K. Bormanis, M. Kalnberga, M. Livinsh, A. Patmalnieks, and A. Sternberg, J. Low Temp. Phys. **117**, 807 (1999).
[5] S.I. Kuroki, M. Toda, M. Umeda, K. Kotani, and T. Ito, ECS Trans. **11**, 293 (2007).
[6] E. Smirnova, A. Sotnikov, H. Schmidt, N. Zaltseva, and M. Weihnacht, Phys. Solid State **51**, 2492 (2009).
[7] T. Wolfram, E. A. Kraut, and F. J. Morin, Phys. Rev. B **7**, 1677 (1973).
[8] B. Stäuble-Pümpin, B. Ilge, V. C. Matijasevic, P. M. L. O. Scholte, A. J. Steinfort, and F. Tuinstra, Surf. Sci. **369**, 313 (1996).
[9] Y. Liang and D. A. Bonnell, Surf. Sci. **310**, 128 (1994).
[10] K. Szot and W. Speier, Phys. Rev. B **60**, 5909 (1999).
[11] P. Chaudhari, R. H. Koch, R. B. Laibowitz, T. R. McGuire, and R. J. Gambino, Phys. Rev. Lett. **58**, 2684 (1987).

[12]V. Ravikumar, D. Wolf, and V. P. Dravid, Phys. Rev. Lett. **74**, 960 (1995).
[13]T. A. Heimer, S. T. D'Arcangelis, F. Farzad, J. M. Stipkala, and G. J. Meyer, Inorg. Chem. **35**, 5319 (1996).
[14]A. Stashans, R. Viteri, and J. Torres, Int. J. Quantum Chem. **106**, 1715 (2006).
[15]M. Kudo, T. Hikita, T. Hanada, R. Sekine, and M. Kawai, Surf. Interface Anal. **22**, 412 (1994).
[16]H. Guhl, W. Miller, and K. Reuter, Phys. Rev. B **81**, 155455 (2010).
[17]B. Hinojosa, T. V. Cleve, and A. Asthagiri, Mol. Simul. **36**, 604 (2010).
[18]R. G. Egdell and P. D. Naylor, Chem. Phys. Lett. **91**, 200 (1982).
[19]L.-Q. Wang, K. F. Ferris, S. Azad, and M. H. Engelhard, J. Phys. Chem. B **109**, 4507 (2005).
[20]L.-Q. Wang, K. F. Ferris, S. Azad, M. H. Engelhard, and C. H. F. Peden, J. Phys. Chem. B **108**, 1646 (2004).
[21]S. Azad, M. H. Engelhard, and L.-Q. Wang, J. Phys. Chem. B **109**, 10327 (2005).
[22]J. A. Rodriguez, S. Azad, L. Wang, J. García, A. Etxeberria, and L. González, J. Chem. Phys. **118**, 6562 (2003).
[23]H. G. Wolfram Miller and K. Reuter, Surf. Sci. **604**, 372 (2010).
[24]M. Khalid, A. Setzer, M. Ziese, P. Esquinazi, D. Spemann, A. Pöppl, and E. Goering, Phys. Rev. B **81**, 214414 (2010).
[25]E. Goering, S. Gold, A. Bayer, and G. Schuetz, J. Synchrotron Radiat. **8**, 434 (2001).
[26]B. Psiuk, J. Szade, H. Schroeder, H. Haselier, M. Młynarczyk, R. Waser, and K. Szot, Appl. Phys. A **89**, 451 (2007).
[27]P. Hohenberg and W. Kohn, Phys. Rev. **136**, B864 (1964).
[28]W. Kohn and L. J. Sham, Phys. Rev. **140**, A1133 (1965).
[29]J. P. Perdew, J. A. Chevary, S. H. Vosko, K. A. Jackson, M. R. Pederson, D. J. Singh, and C. Fiolhais, Phys. Rev. B **46**, 6671 (1992).
[30]G. Kresse and J. Hafner, Phys. Rev. B **47**, 558 (1993).
[31]G. Kresse and J. Furthmüller, Comput. Mater. Sci. **6**, 15 (1996).
[32]P. E. Blöchl, Phys. Rev. B **50**, 17953 (1994).
[33]D. M. Wood and A. Zunger, J. Phys. A **18**, 1343 (1985).
[34]H. J. Monkhorst and J. D. Pack, Phys. Rev. B **13**, 5188 (1976).
[35]S. Ohta, T. Nomura, H. Ohta, M. Hirano, H. Hosono, and K. Koumoto, Appl. Phys. Lett. **87**, 092108 (2005).
[36]I. Shein and A. Ivanovskii, Phys. Lett. A **371**, 155 (2007).
[37]S. Saha, T. P. Sinha, and A. Mookerjee, J. Phys. Condens. Matter **12**, 3325 (2000).
[38]R. T. Gallant and A. St-Amant, Chem. Phys. Lett. **256**, 569 (1996).
[39]R. I. Eglitis, S. Piskunov, E. Heifets, E. A. Kotomin, and G. Borstel, Ceram. Int. **30**, 1989 (2004).
[40]M.-Q. Cai, Y.-J. Zhang, G.-W. Yang, Z. Yin, M.-S. Zhang, W.-Y. Hu, and Y.-G. Wang, J. Chem. Phys. **124**, 174701 (2006).
[41]S. Kimura, J. Yamauchi, M. Tsukada, and S. Watanabe, Phys. Rev. B **51**, 11049 (1995).
[42]X. Zuo, S.-D. Yoon, A. Yang, W.-H. Duan, C. Vittoria, and V. G. Harris, J. Appl. Phys. **105**, 07C508 (2009).
[43]W. A. Adeagbo, G. Fischer, A. Ernst, and W. Hergert, J. Phys. Condens. Matter **22**, 436002 (2010).
[44]J. Osorio-Guillén, S. Lany, S. V. Barabash, and A. Zunger, Phys. Rev. Lett. **96**, 107203 (2006).
[45]S. Gallego, J. I. Beltrán, J. Cerdá, and M. C. Muñoz, J. Phys. Condens. Matter **17**, L451 (2005).
[46]J. Beltrán, C. Monty, L. Balcells, and C. Martínez-Boubeta, Solid State Commun. **149**, 1654 (2009).
[47]H. Peng, H. J. Xiang, S.-H. Wei, S.-S. Li, J.-B. Xia, and J. Li, Phys. Rev. Lett. **102**, 017201 (2009).
[48]S.-C. Li, J.-g. Wang, P. Jacobson, X.-Q. Gong, A. Selloni, and U. Diebold, J. Am. Chem. Soc. **131**, 980 (2009).